

## Phase diagram and critical behavior of the pair annihilation model

This article has been downloaded from IOPscience. Please scroll down to see the full text article.

J. Stat. Mech. (2010) P05009

(<http://iopscience.iop.org/1742-5468/2010/05/P05009>)

View [the table of contents for this issue](#), or go to the [journal homepage](#) for more

Download details:

IP Address: 152.84.71.38

The article was downloaded on 02/07/2010 at 18:44

Please note that [terms and conditions apply](#).

# Phase diagram and critical behavior of the pair annihilation model

Adriana Gomes Dickman<sup>1</sup> and Ronald Dickman<sup>2,3</sup>

<sup>1</sup> Departamento de Física e Química, Pontifícia Universidade Católica de Minas, Gerais, Av. Dom José Gaspar, 500, Coração Eucarístico, 30535-901 Belo Horizonte, Minas Gerais, Brazil

<sup>2</sup> Departamento de Física, ICEx, and Universidade Federal de Minas Gerais, Caixa Postal 702, 30123-970 Belo Horizonte, Minas Gerais, Brazil

<sup>3</sup> National Institute of Science and Technology for Complex Systems, Caixa Postal 702, 30161-970 Belo Horizonte, Minas Gerais, Brazil

E-mail: [adickman@pucminas.br](mailto:adickman@pucminas.br) and [dickman@fisica.ufmg.br](mailto:dickman@fisica.ufmg.br)

Received 3 March 2010

Accepted 20 April 2010

Published 14 May 2010

Online at [stacks.iop.org/JSTAT/2010/P05009](http://stacks.iop.org/JSTAT/2010/P05009)

doi:10.1088/1742-5468/2010/05/P05009

**Abstract.** We study the critical behavior of the pair annihilation model (PAM) with diffusion in one, two and three dimensions, using the pair approximation (PA) and Monte Carlo simulation. Of principal interest is the dependence of the critical creation rate,  $\lambda_c$ , on the diffusion probability  $D$ , in particular, whether survival is possible at arbitrarily small creation rates, for sufficiently rapid diffusion. Whilst the PA predicts that in any spatial dimension  $d \geq 1$ ,  $\lambda_c \rightarrow 0$  at some diffusion probability  $D^* < 1$  Katori and Konno (1992 *Physica A* **186** 578) showed rigorously that, for  $d \leq 2$ , one has  $\lambda_c > 0$  for any  $D < 1$ . Our simulation results are consistent with this theorem. In two dimensions, the extinction region becomes narrow as  $D$  approaches unity. Our results are well described by  $\lambda_c \propto \exp[-\text{const.}/(1 - D)^\gamma]$ , with  $\gamma = 1.43(2)$ . In three dimensions we find  $D^* = 0.340\,53(1)$ . The simulation results confirm that the PAM belongs to the directed percolation universality class.

**Keywords:** phase diagrams (theory), phase transitions into absorbing states (theory), diffusion

**ArXiv ePrint:** [1003.1708](https://arxiv.org/abs/1003.1708)

---

**Contents**

<b>1. Introduction</b>	<b>2</b>
<b>2. The model</b>	<b>3</b>
<b>3. Cluster approximations</b>	<b>5</b>
3.1. One-site approximation . . . . .	5
3.2. Pair approximation . . . . .	6
<b>4. Results</b>	<b>8</b>
4.1. One dimension . . . . .	8
4.1.1. Spreading behavior. . . . .	8
4.2. Two dimensions . . . . .	10
4.2.1. Spreading behavior. . . . .	10
4.2.2. Steady-state behavior. . . . .	10
4.2.3. Quasistationary simulations. . . . .	12
4.2.4. Phase boundary. . . . .	12
4.3. Three dimensions . . . . .	13
4.3.1. Determination of $D^*$ . . . . .	13
4.3.2. Quasistationary simulations. . . . .	14
<b>5. Discussion</b>	<b>15</b>
<b>Acknowledgment</b>	<b>16</b>
<b>References</b>	<b>16</b>

---

**1. Introduction**

In recent decades, general theories of phase transitions and critical phenomena have been elaborated, unifying our understanding of equilibrium phase transitions in fluids, magnets and other systems. In contrast, the study of nonequilibrium critical phenomena is still in development. Since the transition rates in such systems do not satisfy detailed balance, the steady-state probability distribution in these systems is not known *a priori* and the analysis must be based upon the dynamics. Starting from the basic contact process [1], many particle systems have been studied in efforts to characterize scaling properties at nonequilibrium phase transitions [2]–[4]. These models, which involve creation and annihilation of particles on a lattice, typically exhibit a phase transition to an *absorbing state* (one allowing no escape) and so violate the detailed balance principle. An issue that has attracted some interest is the combined effect of multiparticle rules and diffusion (hopping), which tends to spread particles uniformly over the system.

Here we revisit the pair annihilation model (PAM) [2, 5]. In this model particles diffuse on a lattice at a rate  $D$ , nearest-neighbor pairs of particles are annihilated at a rate  $(1-D)/(1+\lambda)$  and particles attempt to create new particles at a rate  $(1-D)\lambda/(1+\lambda)$ . Double occupancy of sites is forbidden. The model exhibits active and absorbing phases, separated by a continuous phase transition at  $\lambda_c(D)$ . Using cluster approximations

and Monte Carlo simulation, we determine the phase boundary in one, two and three dimensions.

The pair approximation predicts that for a diffusion rate greater than a certain value,  $D^*$ , the critical parameter  $\lambda_c = 0$ . (That is, for  $D > D^*$ , an arbitrarily small creation rate is sufficient to maintain a nonzero particle density.) This prediction is known to be wrong in dimensions  $d \leq 2$ : Katori and Konno [6] proved that  $\lambda_c > 0$  for any diffusion probability  $D < 1$ , in one and two dimensions. Their theorem is based on a relation between the PAM and the branching–annihilating random walk of Bramson and Gray [7]. Existence of a  $D^* < 1$  is not ruled out in  $d \geq 3$  dimensions. The difference is connected with the nonrecurrence of random walks in  $d \geq 3$  [6]. The precise manner in which  $\lambda_c$  tends to zero as  $D \rightarrow 1$  is, however, unknown and the numerical value of  $D^*$  in three or more dimensions has not, to our knowledge, been determined. The principal motivation for the present work is to determine  $\lambda_c(D)$  via numerical simulation. We also verify that the model belongs to the directed percolation (DP) universality class, as expected on the basis of symmetry considerations [8]–[10] and numerical simulations [11]. Our simulation results, while consistent with the Katori–Konno theorem, show that, in the two-dimensional case,  $\lambda_c$  becomes extremely small as  $D$  approaches unity, possibly suggesting the (incorrect) impression that the critical value is actually zero at some finite diffusion rate.

The remainder of this paper is organized as follows. In section 2 we define the model and discuss its limiting behaviors in the  $\lambda$ – $D$  plane. Then in section 3 we present, for completeness, the one-and two-site cluster approximations. Numerical results are discussed in section 4, followed by a brief discussion in section 5.

## 2. The model

The PAM is defined on a lattice, in which sites can be either occupied by a particle or vacant [2, 5]; we denote these states by  $\sigma_x = 1$  (site  $x$  occupied) and  $\sigma_x = 0$  (site  $x$  vacant). There are three types of transitions: nearest-neighbor (NN) hopping (‘diffusion’), creation and pairwise annihilation, with associated probabilities  $D$ ,  $(1 - D)\lambda/(1 + \lambda)$  and  $(1 - D)/(1 + \lambda)$ , respectively. (These represent the probability that the next *attempted* transition is of a given kind. The probability of success, of course, depends on the details of the configuration.)

In a hopping transition, a site  $x$  is chosen at random, along with a nearest-neighbor site  $y$  of  $x$ . Then if  $\sigma_x \neq \sigma_y$ , the states are exchanged. In a creation event, a site  $x$  is chosen. If  $\sigma_x = 1$ , a nearest neighbor  $y$  is chosen, and if  $\sigma_y = 0$  this variable is set to one. Finally, in an annihilation event, a site  $x$  is chosen; if  $\sigma_x = 1$ , a nearest neighbor  $y$  is chosen at random, and if  $\sigma_y = 1$ , both variables are set to zero. Each transition corresponds to a time increment  $\Delta t = 1/N_{\text{site}}$ , where  $N_{\text{site}}$  is the number of lattice sites.

To improve efficiency, in simulations site  $x$  is chosen from a list of occupied sites; then the time increment is  $\Delta t = 1/N_p$ , with  $N_p$  the number of *particles* in the system, immediately prior to the transition. (One could, of course, take  $\Delta t$  as an exponentially distributed random variable with mean  $1/N_p$ , but this procedure, although more faithful to the continuous-time nature of the process, is not expected to have any influence on asymptotic scaling properties.) In this implementation, the rate of annihilation of a given NN particle pair is

$$R_{\text{an}} = \frac{1}{\Delta t} \frac{1 - D}{1 + \lambda} \frac{2}{N_p} \frac{1}{2d} = \frac{1 - D}{d(1 + \lambda)} \quad (1)$$

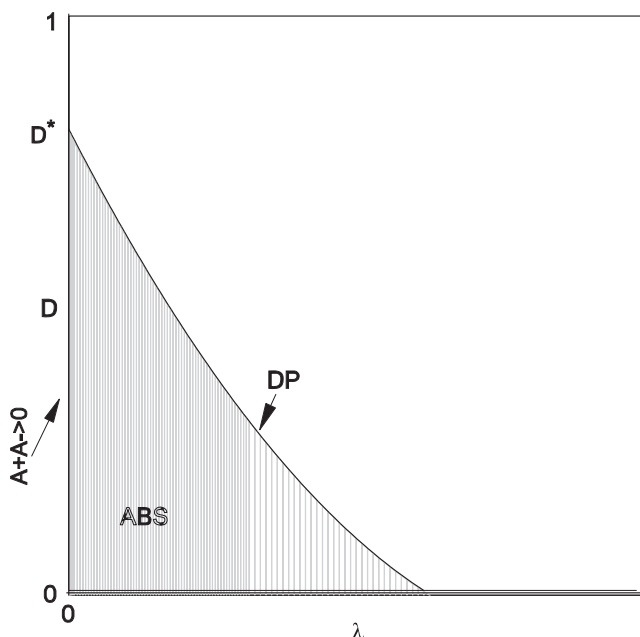


**Figure 1.** Schematic phase diagram of the PAM in the  $\lambda$ - $D$  plane. The results of [6] imply that  $D^* = 1$  in one and two dimensions.

where the factor  $2/N_p$  arises because either particle in the pair can be selected from the list of  $N_p$  particles.

The particle-free configuration is absorbing. By analogy with the contact process [1, 2], we expect that in the infinite-size limit the system undergoes a phase transition between an active state (with nonzero stationary particle density) and an absorbing one, as one crosses the critical line  $\lambda_c(D)$  in the  $\lambda$ - $D$  plane. As creation depends upon a single particle, the order parameter is the stationary density of particles,  $\rho$ . Absorbing state phase transitions belong generically to the DP universality class; this is expected to hold for the PAM, since it possesses no special symmetries or conserved quantities. In fact, the PAM is essentially a continuous-time version of the branching-annihilating random walk (BARW) process with a single offspring, for which DP universality is well established in the one-dimensional case [10, 11].

When a new particle is created, it always forms a pair with the ‘parent’ particle, making these two particles susceptible to annihilation. In the active stationary state, increasing  $D$  at fixed  $\lambda$  tends to reduce the fraction of nearest-neighbor particle pairs toward its random mixing value,  $\rho^2$ . Thus we should expect  $\lambda_c$  to be a decreasing (or, at least, nonincreasing) function of  $D$ . In the simplest mean-field theory analysis, the annihilation rate is proportional to  $\rho^2$ , so that for small  $\rho$  one has  $\dot{\rho} \propto \lambda\rho - \text{const.} \times \rho^2$ , which admits a stationary solution  $\rho \propto \lambda$  for *any* nonzero creation rate. In the limit  $D \rightarrow 1$  we expect mean-field theory to hold, so that  $\lambda_c \rightarrow 0$  in this limit. This raises the question of whether  $\lambda_c$  vanishes at some diffusion probability  $D^*$  strictly less than unity. While the two-site approximation predicts  $D^* < 1$  in any dimension, the results of Katori and Konno [6] imply that  $D^* = 1$  in dimensions  $d \leq 2$ .

The phase diagram of the PAM is expected to have the form shown in figure 1. For  $D < D^*$  the behavior along the critical line  $\lambda_c(D)$  should be that of DP, given that such

behavior is generic for absorbing state phase transitions without special symmetries or conserved quantities [8, 9]. If  $D^* < 1$ , then we expect mean-field-like critical behavior as  $\lambda \rightarrow \lambda_c = 0$  at fixed  $D > D^*$ . Within the absorbing phase, for  $0 < \lambda < \lambda_c(D)$ , an isolated particle can produce an offspring, leading to annihilation of both the original and the new particle. On the line  $\lambda = 0$ , this channel to annihilation is not available and isolated particles cannot disappear. Thus the dynamics at long times, for  $D > 0$ , will be that of the diffusive annihilation process  $A + A \rightarrow 0$ , for which the particle density  $\rho(t)$  decays  $\sim 1/\sqrt{t}$  in  $d = 1$ ,  $\sim (\ln t)/t$  in two dimensions, and  $\sim 1/t$  in  $d \geq 3$  [12, 13].

The dependence on dimension is especially clear on the line  $\lambda = 0$ , when starting with a single pair. The evolution is then described by a lattice random walk  $\mathbf{X}$  (i.e. the separation between the two particles), with the possibility of mutual annihilation when  $|\mathbf{X}| = 1$ . In one and two dimensions, the sites with  $|\mathbf{X}| = 1$  are visited infinitely often, so that annihilation is certain for any  $D < 1$ . In three or more dimensions there is a finite probability that the walk never revisits the neighborhood of the origin, and thus the survival probability approaches a nonzero limiting value as  $t \rightarrow \infty$ . This observation furnishes a basis for determining  $D^*$  in three or more dimensions.

At the point  $D = 1$  the model corresponds to a collection of random walkers (their number is strictly conserved), with double occupancy prohibited, i.e. a symmetric exclusion process on  $\mathbb{Z}^d$ . Finally, at the point  $\lambda = D = 0$ , starting from all sites occupied, pairs are annihilated successively until only isolated particles remain. This is equivalent to the random sequential adsorption (RSA) of dimers. (In the present case, of course, dimers are removed, not adsorbed, so the final particle density is  $1 - 2\theta_\infty$ , where  $\theta_\infty$  is the final coverage in RSA.) On the line, the final density of isolated particles is  $e^{-2} = 0.135\,335\,\dots$  [14], while in two dimensions one has  $\rho_\infty \simeq 0.093\,108(8)$  [15]. One may anticipate interesting crossover behaviors in the vicinity of one or another limit. In the present work, however, we focus on determining the function  $\lambda_c(D)$  using Monte Carlo simulation.

### 3. Cluster approximations

In this section we study the PAM through mean-field site and pair approximations [16]. In general, mean-field results provide a good qualitative description of the phase diagram and give an order-of-magnitude estimate of the critical point.  $n$ -site approximations are a natural way to improve the mean-field approach. The method consists of treating the transitions inside clusters of  $n$  sites exactly, while transitions involving sites outside the cluster are treated in an approximate manner.

#### 3.1. One-site approximation

Let  $\rho = \text{Prob}(\sigma_x = 1)$  denote the density of particles. The density is governed by

$$\begin{aligned} \frac{d\rho}{dt} = & \frac{1}{2d}(1-D)\frac{\lambda}{1+\lambda} \sum_{\hat{e}} P(\sigma_x = 0, \sigma_{x+\hat{e}} = 1) - \frac{1}{d}\frac{1-D}{1+\lambda} \sum_{\hat{e}} P(\sigma_x = 1, \sigma_{x+\hat{e}} = 1) \\ & - D \sum_{\hat{e}} P(\sigma_x = 1, \sigma_{x+\hat{e}} = 0) + D \sum_{\hat{e}} P(\sigma_x = 0, \sigma_{x+\hat{e}} = 1), \end{aligned} \quad (2)$$

where the sums are over the  $2d$  nearest neighbors of site  $x$  and  $P(\sigma_x, \sigma_{x+\hat{e}})$  is a two-site joint probability. Equation (2) couples the one-site probability  $\rho$  to the two-site probabilities, which in turn depend on the three-site probabilities, and so forth, leading to an infinite hierarchy of equations for the  $n$ -site probabilities. The site approximation consists in truncating this hierarchy at  $n = 1$ , so that the two-site probabilities are replaced by a product of two one-site probabilities. Assuming spatial homogeneity and isotropy we obtain the following equation for  $\rho$ :

$$\frac{d\rho}{dt} = \frac{1-D}{1+\lambda} [\lambda\rho - (2+\lambda)\rho^2]. \quad (3)$$

The stationary solutions are  $\bar{\rho} = 0$  (unstable for  $\lambda > 0$ ) and  $\bar{\rho} = \lambda/(2+\lambda)$ . Thus, in this approximation the critical parameter  $\lambda_c$  is zero in any dimension. Notice that in this approximation the diffusion rate has no influence on the stationary solution.

### 3.2. Pair approximation

To derive the pair approximation equations, we consider the changes in the configuration of a NN pair of sites (the *central* pair), given the states of the surrounding sites. Using the symbols  $\circ$  and  $\bullet$  to represent, respectively, vacant and occupied sites, the states of a pair are  $\circ\circ$ ,  $\bullet\bullet$ ,  $\bullet\circ$  and  $\circ\bullet$ ; the latter two have the same probability and may be treated as a single class using appropriate symmetry factors. It is convenient to use  $(\bullet\bullet)$  to denote the fraction of  $\bullet\bullet$  pairs, and so on. Then we have for the site fractions  $(\bullet) = \rho$  and  $(\circ) = 1 - \rho$ :

$$(\bullet) = (\bullet\bullet) + (\bullet\circ), \quad (4)$$

$$(\circ) = (\circ\circ) + (\circ\bullet). \quad (5)$$

The pair fractions satisfy  $(\circ\circ) + 2(\circ\bullet) + (\bullet\bullet) = 1$ . The pair approximation consists in writing the joint probability of a set of three neighboring sites in the form  $(abc) = (ab)(bc)/(b)$ .

There are five possible transitions between the pair states. Consider, for example, the transition  $\circ\circ \rightarrow \circ\bullet$ . This can occur via creation or via hopping if and only if the rightmost site of the central pair has an occupied NN. Since its NN *within* the central pair is vacant, at least one of its  $2d - 1$  NNs *outside* the central pair must be occupied. The rate of transitions via creation is

$$R_{1,c} = (1-D)\tilde{\lambda} \frac{2d-1}{2d} \frac{(\circ\circ)(\circ\bullet)}{(\circ)} \quad (6)$$

where we introduced  $\tilde{\lambda} = \lambda/(1+\lambda)$ . Adding the contribution due to diffusion, we obtain the total rate for this transition:

$$R_1 = \frac{2d-1}{2d} \frac{(\circ\circ)(\circ\bullet)}{(\circ)} [D + (1-D)\tilde{\lambda}]. \quad (7)$$

Note that the contribution to the loss term for  $(\circ\circ)$  associated with this process is  $2R_1$ , due to the mirror transition  $\circ\circ \rightarrow \bullet\circ$ .

The rates for the other transitions are:

$\circ\bullet \rightarrow \circ\circ$ :

$$R_2 = \frac{2d-1}{2d} \frac{(\circ\bullet)}{(\bullet)} [D(\circ\bullet) + 2(1-D)(1-\tilde{\lambda})(\bullet\bullet)] \quad (8)$$

$\circ\circ \rightarrow \bullet\bullet$ :

$$R_3 = \frac{2d-1}{2d} \frac{(\circ\circ)^2}{(\circ)} [D + (1-D)\tilde{\lambda}] + \frac{1}{2d}(1-D)\tilde{\lambda}(\circ\bullet) \quad (9)$$

$\bullet\bullet \rightarrow \circ\circ$ :

$$R_4 = \frac{1}{d}(1-D)(1-\tilde{\lambda})(\bullet\bullet) \quad (10)$$

$\bullet\bullet \rightarrow \circ\bullet$ :

$$R_5 = \frac{2d-1}{2d} \frac{(\bullet\bullet)}{(\bullet)} [2(1-D)(1-\tilde{\lambda})(\bullet\bullet) + D(\circ\bullet)]. \quad (11)$$

The equations of motion for the pair probabilities are then

$$\frac{d}{dt}(\circ\circ) = 2R_2 + R_4 - 2R_1 \quad (12)$$

$$\frac{d}{dt}(\circ\bullet) = R_1 + R_5 - R_2 - R_3 \quad (13)$$

and

$$\frac{d}{dt}(\bullet\bullet) = 2R_3 - R_4 - 2R_5. \quad (14)$$

The active stationary solution of the above equations is

$$\bar{\rho} = \frac{\lambda[(4d-3+D)\lambda - 2(1-2dD)]}{(4d-3+D)\lambda^2 + 2[2d(D+2) - 3]\lambda + 4(2d-1)D}, \quad (15)$$

and

$$\overline{(\bullet\bullet)} = \frac{\lambda}{\lambda+2} \bar{\rho}. \quad (16)$$

For  $\lambda < 2(1-2dD)/(4d-3+D)$ , only the trivial solution ( $\bar{\rho} = 0$ ) exists. If  $D \geq D^* = 1/2d$ , however, the active solution exists for any  $\lambda > 0$ . The phase transition occurs at

$$\lambda_c = \begin{cases} \frac{2(1-2dD)}{4d-3+D}, & D < D^* = \frac{1}{2d} \\ 0, & D > D^*. \end{cases} \quad (17)$$

Thus the pair approximation predicts a nonzero critical creation rate only for diffusion probabilities  $D < D^* = 1/(2d)$ ; for larger values of  $D$ , there is a nonzero particle density for any  $\lambda > 0$ , as in the one-site approximation. For  $D = 0$ , we have  $\lambda_c = 2, 2/5$  and  $2/9$  in one, two and three dimensions, respectively; the corresponding values from simulation are  $\lambda_c = 5.368(1), 1.0156(1)$  and  $0.475(1)$ . (We note that the pair approximation results derived above differ slightly from those given in [2] since in the latter case the annihilation rate for an NN particle pair is taken as  $(1-D)/(1+\lambda)$ , i.e.  $d$  times the rate given in equation (1).)

Katori and Konno [6] proved that the prediction of  $D^* < 1$ , furnished by the pair approximation, is wrong for  $d \leq 2$ . That is, in one and two dimensions,  $\lambda_c > 0$  for any  $D < 1$ . In the following section we investigate how  $\lambda_c$  tends to zero as  $D \rightarrow 1$  in one and two dimensions, and determine  $D^*$  in the three-dimensional case.



## 4. Results

We use Monte Carlo simulations to obtain accurate values of the critical creation rate  $\lambda_c(D)$  and the critical exponents of the PAM in one, two and three dimensions. In the latter case, we determine the diffusion rate  $D^*$  via a random walk analysis.

### 4.1. One dimension

*4.1.1. Spreading behavior.* A well-established method for determining the critical point and certain critical exponents is through the study of the propagation of activity, starting from a localized seed, as proposed long ago by Grassberger and de la Torre [17]. One studies the activity averaged over a large set of trials, all starting from a configuration very close to the absorbing state. Here the initial configuration is that of a single pair of particles at the two central sites of an otherwise empty lattice. Each trial ends when it reaches the absorbing state, or at a maximum time,  $t_{\max}$ , chosen such that the activity never reaches the edges of the system (in any trial) for  $t \leq t_{\max}$ .

For  $\lambda > \lambda_c$  there is a nonzero probability that the process survives as  $t \rightarrow \infty$ ; for  $\lambda \leq \lambda_c$  the process dies with probability one. Of primary interest are  $P(t)$ , the probability of surviving until time  $t$  or greater,  $n(t)$ , the mean number of particles (averaged over all trials), and  $R^2(t)$ , the mean-square distance of particles from the origin. At the critical point these quantities follow asymptotic power laws:

$$P(t) \propto t^{-\delta} \quad (18)$$

$$n(t) \propto t^\eta \quad (19)$$

$$R^2(t) \propto t^{z_{\text{sp}}}. \quad (20)$$

The exponents  $\delta$ ,  $\eta$  and  $z_{\text{sp}}$  satisfy the hyperscaling relation  $4\delta + 2\eta = dz_{\text{sp}}$ , in  $d \leq 4$  dimensions [17]. (We note that  $z_{\text{sp}}$  is related to the usual dynamic exponent  $z$  via  $z_{\text{sp}} = 2/z$ .)

We study activity spreading in one dimension using samples from  $10^6$  or  $2 \times 10^6$  trials for each  $\lambda$  value of interest. The maximum time  $t_{\max} = 15\,000$  for  $D \leq 0.7$ ,  $30\,000$  for  $D = 0.8$  and  $0.9$ , and  $60\,000$  for  $D = 0.95$ . (As  $D$  increases, the asymptotic power-law behavior occurs at ever later times.) To ensure that activity never reaches the borders, we use a lattice size of  $L = 50\,000$  for  $t_{\max} = 15\,000$  and  $L = 80\,000$  for the longer studies. A study performed at a given value of  $\lambda$  is used to generate results for nearby values via sample reweighting [18].

To locate the critical point, we use the criterion of power-law behavior of  $n(t)$ ; figure 2 illustrates the analysis for  $D = 0.3$ . The main graph is a log-log plot of  $n(t)$  showing an apparent power law for  $\lambda = 3.4687$ . The curves for nearby values (specifically  $\lambda = 3.4681$ ,  $3.4684$ ,  $3.4690$  and  $3.4693$ , obtained via reweighting), cannot be distinguished on the scale of this graph, but if we plot  $n^* \equiv n/t^\eta$ , the curves for different  $\lambda$  values fan out (upper inset), with the upward curvature indicating a supercritical value of  $\lambda$  and vice versa.

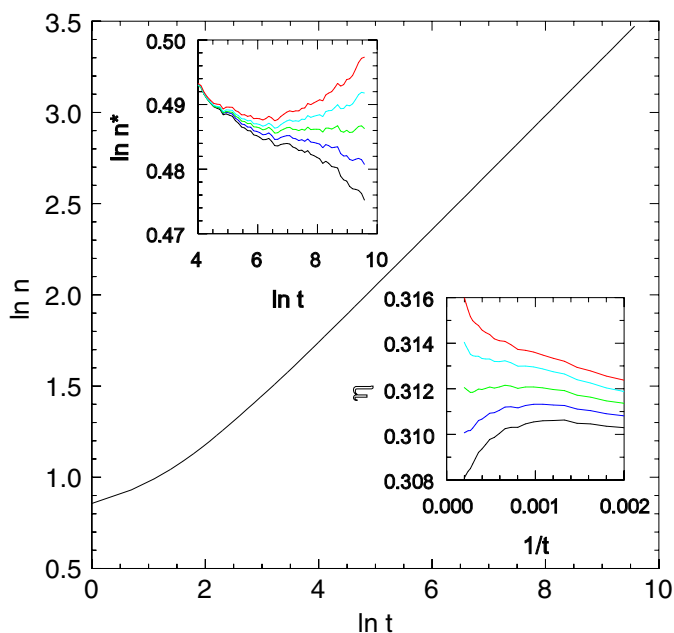


**Figure 2.** Main graph:  $n(t)$  on log scales for the one-dimensional PAM with  $D = 0.3$  and  $\lambda = 3.4687$ . Upper inset:  $n^* = n/t^\eta$  on log scales, for (lower to upper)  $\lambda = 3.4681, 3.4684, 3.4687, 3.4690$  and  $3.4693$ . Lower inset: local slopes  $\eta(t)$  for the same set of  $\lambda$  values.

The exponent  $\eta$  is estimated via analysis of the local slope,  $\eta(t)$ , defined as the inclination of a least-squares linear fit to the data (on logarithmic scales), on the interval  $[t/a, at]$ . (The choice of the factor  $a$  represents a compromise between high resolution, for smaller  $a$ , and insensitivity to fluctuations, for larger values; here we use  $a = 2.59$ .) Plotting  $\eta(t)$  versus  $1/t$  (lower inset of figure 2) allows one to estimate  $\lambda_c$  (the curves for  $\lambda > \lambda_c$  veer upward, and vice versa), and to estimate the critical exponent  $\eta$  by extrapolating  $\eta(t)$  to  $1/t \rightarrow 0$ . The main source of uncertainty in the exponent estimates is the uncertainty in  $\lambda_c$  itself. An analogous procedure is used to estimate exponents  $\delta$  and  $z_{sp}$ .

As expected, we find that the critical parameter,  $\lambda_c(D)$ , becomes smaller with increasing  $D$ . For example,  $\lambda_c(D = 0.0) = 5.3720(5)$ ,  $\lambda_c(D = 0.5) = 2.4473(1)$  and  $\lambda_c(D = 0.95) = 0.3214(1)$ , respectively.

For  $D = 0$ , the critical parameter for the PAM,  $\lambda_c(0) = 5.3720(5)$ , is considerably larger than that of the contact process ( $\lambda_c = 3.29785(2)$ ), as expected since here each annihilation event removes two particles. (The fact that  $\lambda_c$  is *less than twice* the corresponding value in the CP may be attributed to the tendency for particles to cluster: removing two particles may eliminate additional pairs, thus reducing the effective rate of annihilation.)

For all diffusion probabilities studied, our estimates for the critical exponents are in good accord with the DP values  $\delta = 0.15947(3)$ ,  $\eta = 0.31368(4)$  and  $z = 1.26523(3)$  [2]. A plot of the phase boundary in the  $\lambda$ - $D$  plane (see figure 3) suggests that  $\lambda_c \rightarrow 0$  as  $D \rightarrow 1$ , so that  $D^* = 1$ , in agreement with the Katori-Konno theorem. Extrapolation of

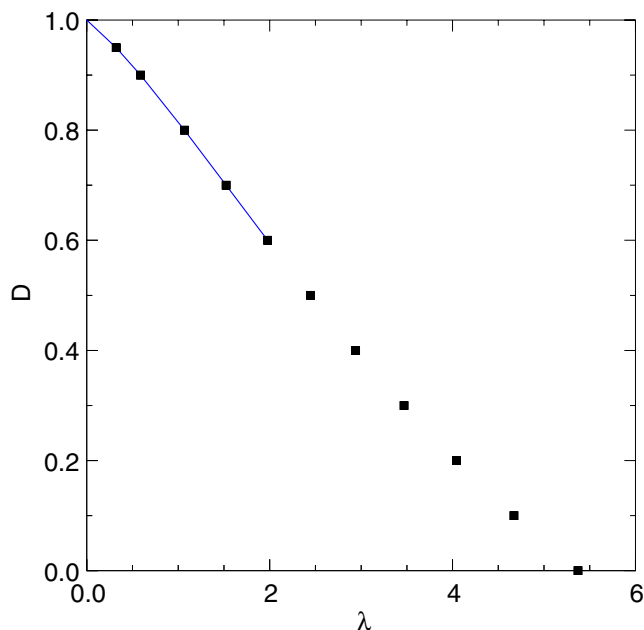


**Figure 3.** Points along the critical line in the  $\lambda$ - $D$  plane in one dimension, as determined via simulation. Error bars are smaller than symbols. The solid line is a quartic fit to the five points with largest  $D$ .

$D$  versus  $\lambda_c$ , using a fourth-order polynomial fit to the data for  $D \geq 0.6$  yields  $D = 1.0005$  for  $\lambda_c = 0$ , confirming to high precision that  $\lambda_c > 0$  for  $D < 1$ .

## 4.2. Two dimensions

*4.2.1. Spreading behavior.* We studied the two-dimensional PAM (on the square lattice) using spreading simulations as described above; results for  $\lambda_c$  are given in table 1. For  $D = 0.7$  the asymptotic power laws are evident only at long times ( $t > 50\,000$  or so); to obtain precise estimates for  $\lambda_c$  the simulations were run to  $t_{\max} = 3 \times 10^5$ . Figure 4 shows that for longer times the curves for  $n(t)$  for different  $\lambda$  values fan out, allowing one to determine  $\lambda_c$ . For  $D = 0.8$ , the largest value studied, we used  $t_{\max} = 3 \times 10^6$  and a lattice size of  $L = 12\,000$ .

*4.2.2. Steady-state behavior.* We use steady-state and quasistationary simulations to investigate the static behavior of the model. In these studies we initialize the system with all sites occupied and allow it to evolve until it attains a quasistationary (QS) regime, in which bulk properties such as the particle density  $\rho$ , averaged over surviving realizations, are time-independent. According to the finite-size scaling hypothesis [19, 20], the QS properties depend on system size  $L$  through the ratio  $L/\xi$ , or equivalently through the scaling variable  $\Delta L^{1/\nu_\perp}$ , where  $\Delta \equiv \lambda - \lambda_c$ . Expressing the order parameter as a function of  $\Delta$  and  $L$ , we have

$$\rho(\Delta, L) \propto L^{-\beta/\nu_\perp} f(\Delta L^{1/\nu_\perp}) \quad (21)$$

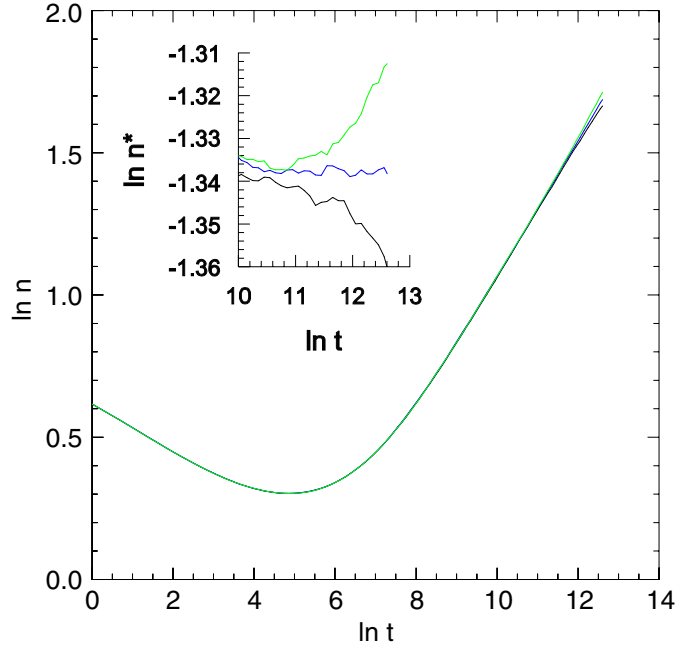


**Figure 4.** Main graph:  $n(t)$  on log scales for the two-dimensional PAM with  $D = 0.7$  and (lower to upper)  $\lambda = 0.00944$ ,  $0.00945$  and  $0.00946$ . Inset:  $n^* = n/t^\eta$  versus  $t$  on log scales.

**Table 1.** Critical creation rate  $\lambda_c(D)$  obtained via spreading, steady-state (SS) and quasistationary (QS) simulations in two dimensions.

$D$	$\lambda_c$		
	Spreading	SS	QS
0.00	1.0156(1)	1.0156(1)	—
0.10	0.7877(1)	0.7875(1)	—
0.20	0.5890(5)	0.5890(5)	—
0.30	0.4167(3)	0.4166(1)	—
0.40	0.2685(5)	0.2685(5)	—
0.50	0.14625(2)	0.1462(2)	—
0.60	—	0.056(1)	0.05632(3)
0.70	0.00945(1)	—	0.00940(5)
0.73	—	—	0.003957(3)
0.78	—	—	0.0004815(7)
0.80	0.000143(1)	—	0.00015(2)

with  $f(x) \propto x^\beta$  as  $x \rightarrow \infty$ . At the critical point,  $\Delta = 0$ ,

$$\rho(0, L) \propto L^{-\beta/\nu_\perp}. \quad (22)$$

Thus an asymptotic power-law dependence of  $\rho$  on  $L$  is a useful criterion for criticality.

We study the QS density as a function of system size to locate the critical point, using sizes  $L = 25, 50, 100, \dots, 800$ . The relaxation time varies from  $\tau = 800$  for the smallest

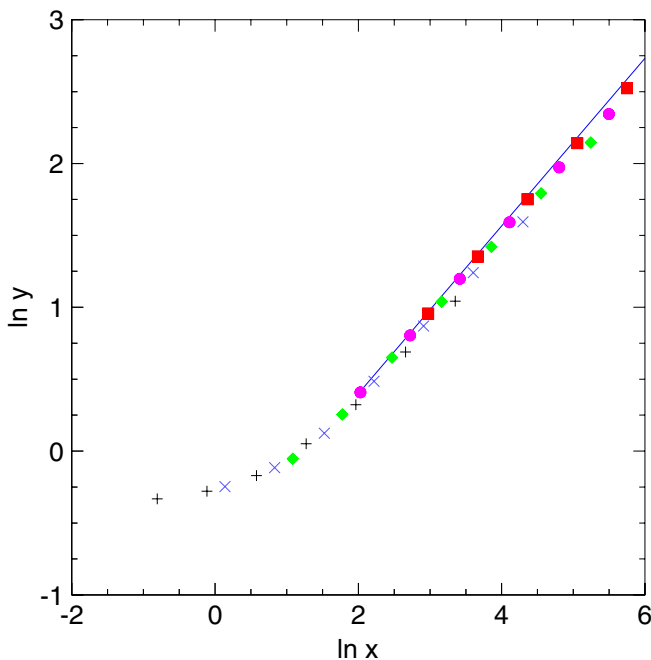


**Figure 5.** Scaling plot of the stationary density in the two-dimensional PAM with  $D = 0$ . System sizes  $L = 16$  (+),  $32$  ( $\times$ ),  $64$  (diamonds),  $128$  ( $\bullet$ ) and  $256$  (squares). The slope of the straight line is  $0.583$ .

size to  $\tau = 200\,000$  for the largest; the number of realizations varies from  $500$  to  $10\,000$ . The results are listed in table 1.

In figure 5 we verify the scaling collapse of the order parameter, plotting  $x \equiv L^{\beta/\nu_{\perp}}\rho$  versus  $y \equiv \Delta L^{1/\nu_{\perp}}$  for system sizes  $L = 16, 32, 64, 128$  and  $256$ . A good collapse is obtained using the DP values  $\nu_{\perp} = 0.733$  and  $\beta/\nu_{\perp} = 0.795$  [2]. The data are consistent with the scaling law  $\rho \propto \Delta^{\beta}$ , using the DP value  $\beta = 0.583(4)$  [2].

*4.2.3. Quasistationary simulations.* We complemented the studies reported above with quasistationary (QS) simulations, which sample directly the QS probability distribution, that is, the long-time distribution conditioned on survival. The details of the method are explained in [21]. To obtain these results we use lattice sizes  $L = 100, 200, 400$  and  $800$  for  $D = 0.7$  and include studies of larger systems for higher diffusion rates (up to  $L = 6400$  for  $D \geq 0.78$ ). The critical point is determined via the criteria of power-law scaling of the density and mean lifetime with system size, and convergence of the moment ratio  $m = \langle \rho^2 \rangle / \rho^2$  to a finite limiting value as  $L \rightarrow \infty$ , as discussed in [22]. (The lifetime  $\tau$  is expected to follow  $\tau \sim L^z$ .) Using this method we obtain the values listed in table 1. We note that our results for  $\beta/\nu_{\perp}$ ,  $z$  and the limiting moment ratio  $m_c$  are consistent with the known DP values of  $0.795(10)$ ,  $1.7674(6)$  and  $1.3257(5)$ , respectively [2, 18, 22].

*4.2.4. Phase boundary.* The results for  $\lambda_c$  obtained using the three simulation approaches are mutually consistent. It appears that for roughly the same computational investment, spreading simulations yield the most precise results. We were unable, however, to

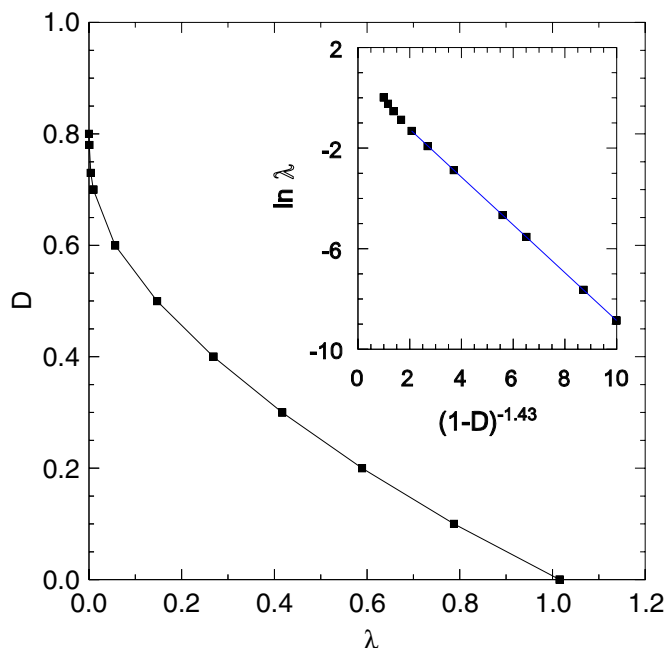


**Figure 6.** Critical line of the two-dimensional PAM. Inset: the same data plotted as  $\ln \lambda_c$  versus  $1/(1 - D)^{1.43}$ .

determine the critical creation rate for  $D > 0.8$  using any of these methods. We estimate, for example, that for  $D = 0.9$ , spreading studies would have to be run to  $t_{\max} \sim 3 \times 10^7$  time steps, with a lattice size  $L \sim 40\,000$ , to yield a useful result, which is beyond our present computational resources.

The available data nevertheless show clearly that  $\lambda_c$  decreases very rapidly with increasing diffusion probability. We find that  $\lambda_c(D)$  can be fitted quite well using an expression of the form

$$\lambda_c = A \exp \left[ -\frac{C}{(1 - D)^\gamma} \right]. \quad (23)$$

Applied to the data for  $D \geq 0.4$ , a least-squares procedure yields  $\gamma = 1.43(2)$ ,  $C = 0.95(2)$  and  $A = 1.9(1)$ . The good quality of the fit is evident in the inset of figure 6. Thus, while a plot of the data on a linear scale might suggest that  $\lambda_c \rightarrow 0$  at some diffusion rate between 0.8 and 1 (see figure 6, main graph), our results are, in fact, consistent with  $\lambda_c$  nonzero, though very small, for diffusion rates between 0.7 and 1.

### 4.3. Three dimensions

*4.3.1. Determination of  $D^*$ .* In three or more dimensions,  $D^*$  can be determined via analysis of the following random walk problem<sup>4</sup>. Consider realizations of the PAM starting with a single pair of particles occupying neighboring sites. As noted in section 2, in  $d \geq 3$ , when  $\lambda = 0$ , there is a finite probability that the particles escape to infinity before they mutually annihilate, so that the survival probability  $P_s(t) \rightarrow P_\infty > 0$  when  $t \rightarrow \infty$ . Now

<sup>4</sup> We thank the referee for suggesting this approach.

suppose that particle creation occurs at a very small rate,  $\lambda \ll 1$ . The initial stage of the evolution is the same as that with  $\lambda = 0$ , but if the pair survives long enough, then at some time  $\tau_c \sim 1/[(1-D)\lambda]$  one of the particles undergoes a creation event. At this point, the two original particles are typically separated by a distance  $\sim \tau_c^{1/2} \gg 1$ , so that the fate of the new pair (parent and offspring) is essentially independent of the other, isolated particle. In the aftermath of the creation event, the population either drops to one (if the new pair annihilates) or increases to three (if they separate before annihilating). At the critical point these outcomes are equally likely, i.e. arbitrarily weak creation causes neither exponential growth nor exponential decay of the survival probability. To determine  $D^*$ , we locate the value of  $D$  such that (with  $\lambda = 0$ ), the original pair escapes to infinity with probability  $P_\infty = 1/2$ .

It is convenient to analyze this problem using a transfer matrix approach. Let  $\mathbf{x}_{1,i}$  and  $\mathbf{x}_{2,i}$  be the positions of the two particles after the  $i$ th event, and let  $\mathbf{X}_i = \mathbf{x}_{2,i} - \mathbf{x}_{1,i}$ , with  $\mathbf{X}_0 = (1, 0, 0)$ .  $\mathbf{X}_i$  is a random walk on  $\mathbb{Z}^3$  with the origin excluded; annihilation is possible only for  $|\mathbf{X}_i| = 1$ . For  $|\mathbf{X}_i| > 1$  the next event is always a jump to a nearest-neighbor site; the six possibilities occur with equal likelihood. For  $|\mathbf{X}_i| = 1$  there are three possible outcomes: annihilation, with probability  $(1-D)/(5D+1)$ , hopping to a nearest neighbor different from the origin, with probability  $D/(5D+1)$  for each of the five possibilities, and no change, with probability  $D/(5D+1)$ . (The latter corresponds to an attempted jump to the origin, which is a reflecting boundary for diffusion.) Organizing these transition probabilities into a transfer matrix, one readily determines the probability distribution  $P(\mathbf{X}_i)$  via iteration.

Using the approach outlined above, we determine the survival probability  $P_{s,i}(D)$  up to  $i = 500$ , using double-precision arithmetic. To extrapolate  $P_\infty(D)$  from these results, we note that at long times the density in the vicinity of the origin decays  $\sim i^{-3/2}$ , so that the dominant correction term decays  $\sim i^{-1/2}$ . We therefore fit the data for  $P_{s,i}$  versus  $i^{-1/2}$  (for  $i \geq 100$ ) with a quadratic polynomial. (Using a higher-order fit yields no significant change.) Finally, interpolating the resulting estimates for  $P_\infty(D)$  yields  $D^* = 0.340\,53(1)$ . This is consistent with an estimate obtained via spreading simulations:  $D^* = 0.3404(12)$ . To within numerical precision we have  $D^* = \pi_3$ , where  $\pi_3 = 0.340\,537\,329\,544 \dots$  is the probability that the simple random walk on  $\mathbb{Z}^3$  returns to the origin [23]. We have not, however, found an argument demonstrating equality of  $D^*$  and  $\pi_3$ .

*4.3.2. Quasistationary simulations.* We employed quasistationary simulations to determine  $\lambda_c(D)$  for the PAM on the simple cubic lattice (see table 2 and figure 7). For relatively small diffusion rates, good results are obtained using lattice sizes  $L = 8, 16, 24, 36$  and  $54$ . For diffusion rates greater than about  $0.25$ , however, there are substantial finite-size effects, and to observe clear signs of DP-like scaling we need to study larger systems ( $L = 80$  and  $120$  for  $D = 0.32$ , and up to  $400$  for  $D = 0.33$ ). As shown in the inset of figure 7,  $\lambda_c$  appears to approach zero via a power law:

$$\lambda_c \sim (D^* - D)^\kappa, \quad (24)$$

with  $\kappa = 1.358(3)$ . The critical exponents determined via finite-size scaling analysis,  $\beta/\nu_\perp = 1.40(1)$  and  $z = 1.94(2)$ , are once again in good agreement with the literature values of  $1.39(3)$  and  $1.919(4)$ , respectively [2]. Our study yields the moment ratio value  $m = 1.47(1)$  for three-dimensional models in the DP universality class; to our knowledge

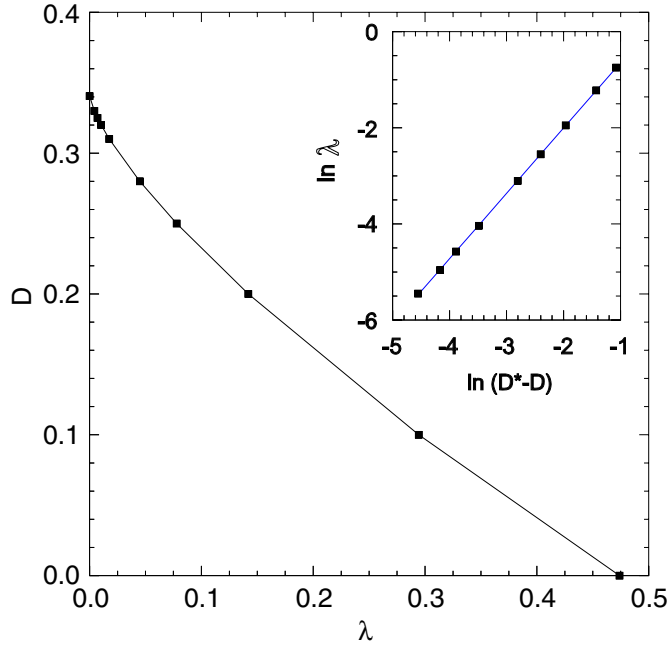


**Figure 7.** Critical line of the PAM in three dimensions; error bars are smaller than symbols. Inset:  $\lambda_c$  versus  $D^* - D$  on log scales; the slope of the straight line is 1.358.

**Table 2.** Critical parameters obtained through quasistationary simulations in three dimensions.

$D$	$\lambda_c$
0.0	0.47390(5)
0.1	0.2943(1)
0.2	0.1420(1)
0.25	0.07790(5)
0.28	0.04487(3)
0.31	0.01762(2)
0.32	0.0103(1)
0.325	0.00703(1)
0.33	0.00430(5)

this quantity has not been determined previously. For  $D > D^*$ , the particle density is expected to tend to zero linearly with  $\lambda$ , as the reproduction rate approaches zero. We verified this behavior (down to  $\lambda = 10^{-4}$ ) for  $D = 0.8$ .

## 5. Discussion

We study the phase boundary of the pair annihilation model in the reproduction rate–diffusion probability ( $\lambda$ – $D$ ) plane. Our simulation results are consistent with the theorem proven some time ago by Katori and Konno [6], namely that in one and two dimensions,  $\lambda_c > 0$  for any  $D < 1$ . The pair approximation is in conflict with this result, as it



predicts that, in any number of dimensions, there is a diffusion probability  $D^* < 1$ , above which  $\lambda_c = 0$ . In one dimension the behavior (in simulations) is straightforward, as  $\lambda_c \propto 1 - D$  for  $D \simeq 1$ . In two dimensions, however, it is quite subtle, as  $\lambda_c$  becomes exponentially small as  $D \rightarrow 1$ , and a cursory analysis could well give the impression that  $\lambda_c$  is actually zero at some value of  $D$  between 0.8 and 1. Finally in three dimensions we find  $D^* = 0.340\,53(1)$  via analysis of a random walk problem. (In this case the pair approximation yields  $D^* = 1/6$ .) For  $D < D^*$ , our data are well described by a power law,  $\lambda_c \sim (D^* - D)^\kappa$ . Intuitively, the unusual behavior of  $\lambda_c(D)$  in two dimensions can be understood as a consequence of  $d = 2$  marking a critical dimension for the recurrence of a random walk. Our simulation results for critical exponents and the moment ratio  $m$  are consistent with the directed percolation values, as expected. Given the qualitative failure of the pair approximation in one and two dimensions, it is natural to ask whether approximations using larger clusters would predict the phase diagram correctly. This strikes us as unlikely, since cluster approximations have been found to be insensitive to subtle effects involving diffusion and/or multiparticle rules in other cases [16, 24, 25].

Finally, we note that our fits to the data for  $\lambda_c(D)$  in two and three dimensions involve power-law exponents, denoted  $\gamma$  and  $\kappa$ , respectively. Since there is no theoretical basis for the fitting forms (equations (23) and (24)), we have no reason to expect these exponents to be universal. Some insight into this question might be gained from studies of the model on other two- and three-dimensional lattices (as well as on the four-dimensional hypercubic lattice), a task we defer to future studies.

## Acknowledgment

RD acknowledges financial support from CNPq, Brazil.

## References

- [1] Harris T E, 1974 *Ann. Probab.* **2** 969
- [2] Marro J and Dickman R, 1999 *Nonequilibrium Phase Transitions in Lattice Models* (Cambridge: Cambridge University Press)
- [3] Henkel M, Hinrichsen H and Lübeck S, 2008 *Nonequilibrium Phase Transitions* (Berlin: Springer)
- [4] Ódor G, 2008 *Universality in Nonequilibrium Lattice Systems* (Singapore: World Scientific)
- [5] Dickman R, 1989 *Phys. Rev. B* **40** 7005
- [6] Katori K and Konno N, 1992 *Physica A* **186** 578
- [7] Bramson M and Gray L, 1985 *Z. Wahrscheinlichkeitstheor. Verwandte Geb.* **68** 447
- [8] Janssen H K, 1981 *Z. Phys. B* **42** 151
- [9] Grassberger P, 1982 *Z. Phys. B* **47** 365
- [10] Cardy J L and Täuber U C, 1998 *J. Stat. Phys.* **90** 1
- [11] Jensen I, 1993 *Phys. Rev. E* **47** R1
- [12] Torney D C and McConnell H E, 1983 *Proc. R. Soc. A* **387** 147
- [13] ben-Avraham D and Havlin S, 2000 *Diffusion and Reactions in Fractals and Disordered Systems* (Cambridge: Cambridge University Press)
- [14] Flory P J, 1939 *J. Am. Chem. Soc.* **61** 1518  
Widom B, 1966 *J. Chem. Phys.* **44** 3888  
Widom B, 1973 *J. Chem. Phys.* **58** 4043
- [15] de Oliveira M J, Tomé T and Dickman R, 1992 *Phys. Rev. A* **46** 6294
- [16] ben-Avraham D and Köhler J, 1992 *Phys. Rev. A* **45** 8358
- [17] Grassberger P and de la Torre A, 1979 *Ann. Phys. NY* **122** 373
- [18] Dickman R, 1999 *Phys. Rev. E* **60** R2441
- [19] Fisher M E, 1971 *Proceedings of the Enrico Fermi International School of Physics* vol 51, ed M S Green (Varenna: Academic)  
Fisher M E and Barber M N, 1972 *Phys. Rev. Lett.* **28** 1516

- [20] Barber M N, 1983 *Phase Transitions and Critical Phenomena* vol 8, ed C Domb and J L Lebowitz (New York: Academic)
- [21] de Oliveira M M and Dickman R, 2005 *Phys. Rev. E* [71 016129](#)
- [22] Dickman R and Leal da Silva J K, 1998 *Phys. Rev. E* [58 4266](#)
- [23] Durrett R, 1991 *Probability: Theory and Examples* (Pacific Grove, CA: Wadsworth and Brooks/Cole)
- [24] Ferreira A A and Fontanari J F, 2009 *J. Phys. A: Math. Theor.* [42 085004](#)
- [25] Ódor G and Dickman R, 2009 *J. Stat. Mech.* [P08024](#)